Fluorescence transient and optical free induction decay spectroscopy of pentacene in mixed crystals at 2 K. Determination of intersystem crossing and internal conversion rates

Vries, Harmen de; Wiersma, Douwe A.

Published in:
The Journal of Chemical Physics

DOI:
10.1063/1.438845

Publication date:
1979

Fluorescence transient and optical free induction decay spectroscopy of pentacene in mixed crystals at 2 K. Determination of intersystem crossing and internal conversion rates

Harmen de Vries and Douwe A. Wiersma

Laboratory for Physical Chemistry, State University, Nyenborgh 16, 9747 AG Groningen, The Netherlands
(Received 23 January 1979)

In this paper the recently reported fluorescence transient, appearing during the onset of cw dye laser excitation of the energetically lower sites of pentacene in *p*-terphenyl at 2 K, is analyzed quantitatively. The role of the lowest triplet state in causing the long (compared to the fluorescence lifetime) transient, is firmly established. For the lower sites a kinetic analysis yields a $T_1 \leftarrow S_1$ intersystem crossing (ISC) yield of about 0.4% and an $S_0 \leftarrow T_1$ ISC rate of $(2.2 \pm 0.1) \times 10^4$ s^{-1}. Using these data in calculating the $S_1 \leftarrow S_0$ transition dipole moment from our earlier OFID experiments yields for the O_1 site (proto) $\mu = 0.71 \pm 0.24$ D. The $S_0 \leftarrow S_1$ internal conversion yield is estimated to be 22%. The fluorescence transients of the energetically higher sites of pentacene in *p*-terphenyl exhibit a much faster decay, which indicates a drastic increase in ISC yield from S_1. Optical free induction decay (OFID) experiments performed on these sites confirm this and imply that the $T_1 \leftarrow S_1$ ISC yield for these sites is ~60%. We further discuss results of an OFID experiment on pentecene in naphthalene and derive in this case at $T_1 \leftarrow S_1$ ISC yield of $\lesssim 2.8\%$ and an $S_0 \leftarrow S_1$ internal conversion yield of $31.5 \pm 1.5\%$. The off-resonance pumping effect in a 3-level system was also studied, using the parameter values for pentacene in *p*-terphenyl. For the lower sites, with the excitation intensities used (~1 MW/m^2) the part of the inhomogeneous absorption line that is pumped has a width of about 2.5 GHz (effective excitation bandwidth < 1 MHz).

I. INTRODUCTION

Recently we reported on the transient (~ 20 μs) in the fluorescence of the energetically lowest site of pentacene in *p*-terphenyl observed during the onset of cw dye laser excitation.[1] Evidence was presented which showed that this transient is caused by a triplet-state bottleneck in the optical pumping cycle.

In this paper a detailed analysis will be given of the transient, yielding a value for the intersystem crossing (ISC) rate from the lowest excited singlet state S_1 to the lowest triplet state T_1. A preliminary account of this work was given in Ref. 2.

The fluorescence transient to be discussed was first observed by Zewail and co-workers[3,4] using the laser frequency switching technique.[5] It was interpreted by them as being due to the decay of so called *molecular eigenstates*,[3] excited prior to the frequency switch. Note that the time constant of the transient is about three orders of magnitude longer than the fluorescence lifetime (τ_{f1}), measured previously by pulsed laser excitation.[6,7] The same authors recently published results on this transient using an acousto-optic modulator (AOM) technique (similar to the method described in Ref. 1) and concluded that the prepared state was *mostly* singlet.[8]

In this context it is important to consider the question, which molecular state will be prepared in the condensed phase, of a guest molecule in an "inert"[9] host lattice at low temperature.

The problem of state preparation is a main issue in the theory of molecular electronic radiationless transitions (for recent reviews, see Refs. 10–12). For the answer to our question several studies concerning medium effects on radiationless transitions are of importance.[9,13–18] It was shown, for example, that molecules belonging to the small or the intermediate cases under isolated conditions behave statistically when the surrounding medium induces fast vibrational relaxation. On the other hand, the "inert" medium was shown to have a negligible effect on the radiationless relaxation rate (after short pulse excitation) of molecules, which showed statistical limit behavior under isolated conditions.[9,17] Due to the fast vibrational relaxation in the high pressure gas phase or the condensed phase, the molecular eigenstates are considerably homogeneously broadened.

Taking into account the information on vibrational relaxation and additional dephasing, known at present, (e.g., Refs. 19 and 20) it seems fairly impossible to excite, in the condensed phase, individual eigenstates or small groups of them, as their widths will overlap.

The statement just made has already been confirmed by experimental results, recently obtained by the photochemical hole burning technique.[19,20] In these molecular mixed crystal experiments at 2 K, the $S_1 \leftarrow S_0$ transition of the respective guest molecules was excited with cw dye laser radiation with a bandwidth, narrow compared to the homogeneous width $1/\pi T_2 = 1/2\pi\tau_{f1}$[21] where T_2 is the decay time of the off-diagonal elements of the density matrix and τ_{f1} was deduced from pulsed laser experiments. It followed, that at 2 K the homogeneous widths of the $S_1 \leftarrow S_0$ transitions under study were precisely determined by τ_{f1}. In other words, the narrow band excitation prepared the vibrationless lowest excited singlet state S_1.

Also in the case of pentacene in *p*-terphenyl at 2 K the lowest excited singlet state is prepared, irrespective of the excitation bandwidth used. This is confirmed by the recent coherent transient experiments, where T_2 was measured. The photon echo (using pulsed dye lasers)[7] and optical free induction decay (OFID) (<1

 0021-9606/79/125807-16$01.00

MHz effective cw dye laser bandwidth)[1] experiments yielded identical results. Note that at 2 K, $T_2 = 2\tau_{f1}$.[21]

The fluorescence transient for the energetically lower sites (O_1, O_2) therefore can be described in terms of a simple picture of singlet and triplet electronic levels. This is done in Sec. III and it follows that the transient behavior can be exploited to determine the (effective) $T_1 \leftarrow S_1$ and $S_0 \leftarrow T_1$ ISC rates. The three-level optical pumping cycle problem, described by Di Bartolo,[22] is extended to include our specific excitation conditions. The inclusion of the three triplet spin sublevels, yielding an effective five-level system, is discussed in Appendix A.

The energetically higher sites of pentacene in p-terphenyl (O_3, O_4) (proto and perdeutero) were also studied. They show a markedly different fluorescence behavior, although they are separated from the O_1 site by only 123 and 182 cm^{-1} (O_3 and O_4 proto, respectively).[23] Based upon the results obtained from the lower and the higher sites, in Sec. V the radiationless relaxation properties of the lowest excited singlet and triplet state are discussed.

Preliminary results of the work described in this paper were already used for the interpretation of the experimental OFID results[1] from the lower sites of pentacene in p-terphenyl.[24] This resulted in a determination of the $S_1 \leftarrow S_0$ transition dipole moment. In Sec. IV an observation of OFID from pentacene in naphthalene at 2 K is reported and discussed. In Sec. IV we also report an OFID experiment on the lower and the higher sites of pentacene in p-terphenyl, using a recently published extracavity laser-frequency switching technique.[25] The result is a beautiful illustration of the influence of the intermediate triplet state (via the A factor[24]) on the decay time of the optical free induction of molecular $S_0 \leftarrow S_1$ transitions.

II. EXPERIMENTAL

A. cw dye laser set-up

The fluorescence experiments were done with the experimental set-up, shown schematically in Fig. 1. It is similar to the one used to obtain the transients, depicted in Ref. 1. For the experiments, described in the present paper, we used as a pump laser a Spectra Physics model 165 or a Control Laser model 554A Arion laser. The cw single mode dye laser is the Spectra Physics model 580 (dye cell type). About 10% of the dye laser beam, which is polarized vertically and has a diameter of ~3 mm, is deflected by a microscope glass G into a confocal interferometer I (Tropel model 240 spectrum analyzer, 1.5 GHz FSR). The light passing the interferometer, as detected by a photodiode, is displayed on an oscilloscope (OSC_1) as a function of frequency. In this way the single mode of the dye laser is monitored. In Fig. 1 INT. STAB. denotes the intensity stabilizer, working independently of the laser.[26] The laser light passes a Lasermetrics model 3030-3 XW electro-optic modulator (bandwidth 100 MHz) (denoted by LM) and a "vertical" polarizer (Rofin). Then 10% of the intensity is deflected by a beam splitter (Perkin Elmer) to a photodiode PD (Monsanto MD2). The photodiode output is compared with a reference voltage, whereupon a feedback signal is going to LM, acting as a polarization rotator. In this way, within a bandwidth of 150 kHz, intensity instabilities are reduced to about 0.5%. This intensity stabilizer also allows the exciting intensity to be easily varied accurately. AOM denotes an acousto-optic modulator (SORO M 30 M). In the configuration used here the acousto-optic crystal ($PbMoO_4$) was placed between two 25 cm lenses, and the optical pulse, emerging from the modulator in first order, was measured to have a rise and fall time of 30 ns (10%–90%). The first order beam from the AOM passes a pinhole P of 1.45 mm diameter and is focused by the 10.0 cm lens L_1 on the sample crystal S.

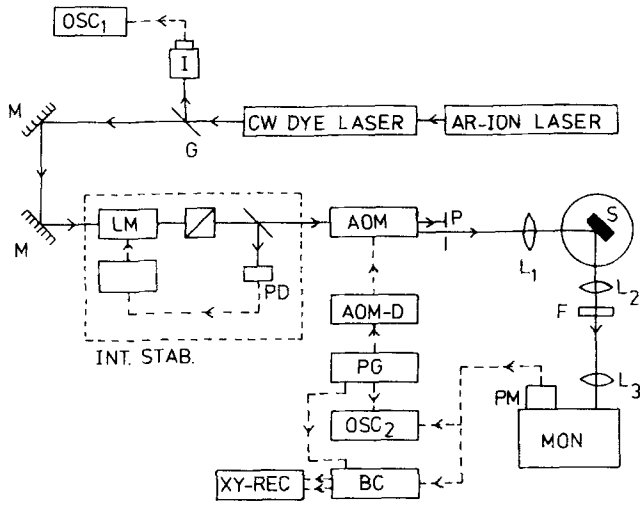

FIG. 1. Experimental set-up, used to obtain the fluorescnece transients, appearing during the onset of the single mode dye laser excitation. Flat mirrors are denoted by M. The remaining abbreviations are explained in the text.

TABLE I. Excitation and detection wavelengths of the pentacene sites in p-terphenyl at 2 K. $1/\lambda_{vac}$ denotes the wavenumber in vacuum. Excitation occurred in the respective origins, while vibronic line fluorescence was detected.

			Excitation		Detection
Site	proto	perdeutero	λ_{air} (Å)	$1/\lambda_{vac}$ (cm^{-1})	λ_{air} (Å)
O_1	×		5921.6	16882.8	6365
O_2	×		5920.1	16887.0	6365, 6449
O_2		×	5911.2	16912.5	6435
O_3	×		5878.7	17005.8	6401
O_3		×	5869.8	17031.7	6385
O_4	×		5858.4	17064.9	6376
O_4		×	5849.4	17091.0	6361

During the experiments the sample was immersed in liquid helium in a glass Dewar that was pumped below the λ point. The emission was detected at right angle, through lenses L_2 and L_3, filter F (Corning 2-60) which blocked the exciting light, and monochromator MON ($\frac{3}{4}$ m Spex model 1702). The different excitation and detection wavelengths used in these experiments, are collected in Table I. The fluorescence detection was

performed with wide monochromator slits (~ 700 μ) to transmit the total emission of the vibronic line detected [see Eq. (12)]. Sometimes the resonantly scattered laser light was monitored. Then the filter F was removed and the monochromator slits were nearly closed (~ 10 μ).

The detector PM is a water-cooled photomultiplier (EMI 9659). The PM signal is fed into either a 7 nsec rise time oscilloscope OSC_2 or a boxcar integrator BC (PAR model 162), both with an input resistance of 50 Ω. The boxcar output is read out into an XY recorder. The synchronization in the experiment is given by a usual laboratory pulse generator PG, delivering 5 V pulses to the SORO AOM driver AOM-D, whereupon 200 MHz RF wave trains are fed to the acousto-optic crystal. In this way light pulses are deflected by the acousto-optic crystal into first order, of 80 μs duration and a repetition rate of 1.27 kHz.

The excitation (peak) power was measured between P and L_1, using a Spectra Physics model 404 power meter. It was determined while deflecting the light continuously through the pinhole P, which could be done by simply feeding 5 V dc into the AOM-D.

B. Fluorescence lifetime experiments

The fluorescence lifetimes of the pentacene O_3 and O_4 sites (proto and perdeutero) at 2 K were measured after excitation by a Molectron DL 200 pulsed dye laser into the respective origins. The vibronic fluorescence was detected using a Spex 1702 monochromator and a fast photomultiplier (RCA 7265, 3 ns rise time). The signal was displayed on the screen of a Tektronix R 7912 transient digitizing system (risetime 0.7 ns). This screen was first calibrated using an Ortec 425 A delay module. We note here that the apparatus used in this lifetime experiment is the same as that used in Ref. 7.

Furthermore the fluorescence lifetime of the O_1 site (proto) was measured as a function of temperature in the range 39–110 K. In this experiment the sample was mounted in a small flow-cryostat (Oxford Instruments) through which cold He gas was pumped. The temperature could be varied by changing the pumping speed, and was measured with a calibrated Au(0.03% Fe)–chromel thermocouple (Oxford Instruments), using liquid He (4.2 K) as a reference.

C. Absorption and OFID experiments, with sample characteristics

Absorption spectra at 2 K of the origins of the different pentacene sites (proto and perdeutero) in the sample that was used in the AOM–fluorescence experiments, were measured. The exciting light emerged from a 30 W Philips lamp (model 6102 M) and a small Bausch and Lomb monochromator ("Catalog no. 33-86-07"). The spectra were recorded using a 1 m Spex 1704 monochromator (~ 0.1 cm^{-1} resolution).

Finally an OFID experiment was performed on the O_1 and O_3 sites (proto) at 2 K, using the extracavity laser-frequency switching technique, recently reported by De Bree and Wiersma.[25] Before entering the Inrad electro-optic crystal, in our case the light passed the intensity stabilizer described above. Moreover the light passed the Inrad crystal only twice, giving a frequency shift of about 500 MHz.

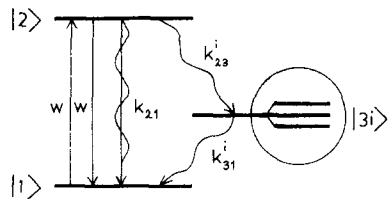

FIG. 2. Molecular model system. The meaning of the energy levels is discussed in the text. Straight and wavy arrows indicate radiative and radiationless transitions, respectively. The part within the circle has a greatly magnified (~ 10^4) energy scale.

The crystals of pentacene -h_{14} and -d_{14} in p-terphenyl, used in the experiments just described, were cut (ab cleavage plane) from the same "mother" crystals as those used in the photon-echo measurements of Refs. 6 and 7. The samples were mounted with the crystal b axis parallel to the polarization direction of the exciting laser. For the pentacene concentration see Appendix B. The thickness of the sample used in the AOM fluorescence experiments was 0.59 ± 0.05 mm.

III. THEORY

A. Model system

As discussed in Sec. I, the fluorescence–transient experiments can be explained in terms of a simple energy level diagram. This level scheme is displayed in Fig. 2 and was also used to derive molecular OFID theory.[24] k_{21} is the total decay rate (radiative and radiationless) from the vibrationless lowest excited singlet state $|2\rangle$ to the singlet ground state $|1\rangle$. k^i_{23} is the radiationless decay rate from $|2\rangle$ to spin-sublevel i of the vibrationless lowest triplet state $|3\rangle$ (i stands for x, y or z). Levels $|3i\rangle$ decay radiationlessly to the ground state (rates k^i_{31}) (from pentacene in p-terphenyl at low temperature no phosphorescence has been observed). The laser is tuned in resonance with the $|2\rangle \leftrightarrow |1\rangle$ transition. w is the absorption rate, which is equal to the rate of induced emission.

For the low temperature solid this is a realistic model system, as here the vibrational relaxation rates are much higher than the rates denoted in Fig. 2. For this reason no excited vibrational levels of states $|1\rangle$ or $|3i\rangle$ are considered, which are populated from $|2\rangle$. A higher electronic triplet state, possibly lying below $|2\rangle$, is also not taken into account, as we assume a very fast internal conversion to the lowest triplet state.[27] Finally, absorption of laser radiation from levels $|2\rangle$ and $|3i\rangle$ may take place. The levels so reached are depleted very fast by vibrational relaxation and can be left out of consideration.

B. Kinetic approach

We prefer here a population kinetic treatment instead of a more general one in terms of the density matrix.

As the region of time we are interested in, is about three orders of magnitude longer than T_2, this way of treating the problem is justified. A comparison with related theories is made in Sec. III C.

In principle, we are concerned with a five-level system (3 $|3i\rangle$ levels). Recently the populating probabilities and decay rates of the triplet spin sublevels of pentacene in p-terphenyl at 77 K have been determined,[28] as already mentioned in Ref. 24. As these values were preliminary,[28] it seemed reasonable to us to perform our simulations of the observed fluorescence transients by considering only *one* intermediate triplet level. This agrees quite well with the real situation, as in many molecules studied, in which one $|3i\rangle$ sublevel is dominantly populated (also in pentacene, according to the preliminary experimental results[28]).

We then have to treat just a three-level system. Here it is assumed that at the temperature the experiments were performed (1.8 to 2 K), spin–lattice relaxation within the $|3i\rangle$ manifold is negligibly slow compared to the other rates in the system (low temperature limit[24]). The three-level population kinetics have been solved by Di Bartolo,[22] using Laplace transformation techniques.

One has to start with the following set of equations of motion:

$$N_1 + N_2 + N_3 = N_0 , \tag{1}$$

$$\dot{N}_2 = -(k_{21} + k_{23})N_2 + w(N_1 - N_2) , \tag{2}$$

$$\dot{N}_3 = k_{23}N_2 - k_{31}N_3 . \tag{3}$$

Here N_1, N_2, and N_3 are the populations of levels $|1\rangle$, $|2\rangle$, and $|3\rangle$, respectively. N_0 is the total number of molecules. The dot denotes the time derivative of N_2 and N_3, respectively. Now, as in the experiment the fluorescence from $|2\rangle$ is monitored, we have to solve these equations for $N_2(t)$. Note that the fluorescence is detected nonresonantly with the laser wavelength. Thus vibrational levels of the ground state are used experimentally, although they need not be considered theoretically. We assume a rectangular excitation pulse of length t_1, starting at $t=0$.

According to Ref. 22, the solution is (for $t<t_1$)

$$N_2(t) = wN_0(c_0 + c_1 e^{s_1 t} + c_2 e^{s_2 t}) . \tag{4}$$

Here s_1 and s_2 are the roots of the equation

$$(K_2 + 2w + s)(k_{31} + s) + wk_{23} = 0 , \tag{5}$$

where $K_2 \equiv k_{21} + k_{23}$. The coefficients c_0, c_1, and c_2 can be obtained using the theory of partial fractions.[29] For example

$$c_1 = \left(\frac{k_{31} + s}{s(s - s_2)}\right)_{s=s_1} . \tag{6}$$

The five-level population kinetics will be treated in Appendix A.

We now have to take into account our experimental situation. First, the effective bandwidth of the exciting light (Sec. III E) was narrow compared to the homogeneous width of the pentacene $|2\rangle \leftrightarrow |1\rangle$ transition (7 MHz for the O_1 and O_2 sites[1,7]). As a consequence, the simple expression with the Einstein B coefficient cannot be used for the induced transition rate w. Second, the effective excitation bandwidth was very narrow compared to the inhomogeneous width of the transition (0.7 cm^{-1} = 21 GHz [O_1 site (proto)], which means that the final theoretical result has to be integrated over the inhomogeneous lineshape.

We proceed by deriving the appropriate expression for w. We approximate the exciting radiation field by considering it to be perfectly monochromatic (angular frequency ω) and linearly polarized (polarization σ) (Sec. III E). Also its intensity is supposed to be constant (Sec. III E). When the molecular transition interacting with the radiation field is infinitely sharp (angular frequency ω_0), one can, in the long time limit, derive for w the following expression[30]:

$$w_{t\to\infty} = \frac{\pi\omega_0}{\hbar\epsilon_0 L^3} |\hat{e}_\sigma \cdot \mu|^2 n_\sigma \delta(\omega - \omega_0) . \tag{7}$$

Here $\hbar$ is Planck's constant over 2π, and ϵ_0 is the permittivity of free space. The molecule and field are assumed to be contained in a cubic cavity of volume L^3 and $\hat{e}_\sigma$ is a unit vector specifying the polarization direction. μ is the transition dipole moment and n_σ is the number of photons in the excited mode of the radiation field.

We wish to make a comment here on the limit $t\to\infty$, taken in the derivation of Eq. (7), which leads to the delta function $\delta(\omega - \omega_0)$.[30] For short times off-resonance pumping of the infinitely sharp transition (meaning that $\omega \neq \omega_0$) will be possible. For long times, however, the delta function only allows resonant excitation. This may be interpreted as being due to a width $\Delta\omega$ in the molecule-field interaction, related by the uncertainty principle to the short period of time Δt after the onset of this interaction. We assume the long time limit formula to hold in the time region of interest in our experiments (Sec. III E).

We have further to take into account the homogeneous width of the excited transition (Ref. 31, p. 133), which, in our case, has the (normalized) Lorentzian line shape:

$$\frac{1}{\pi T_2} \frac{1}{(\omega_0 - \bar{\omega}_0)^2 + \left(\frac{1}{T_2}\right)^2} .$$

The meaning of T_2 and ω_0 was given before. $\bar{\omega}_0$ is the homogeneous line center. Of course the introduction of this formula imposes a second time limit upon the validity of the w formula obtained hereafter, namely, its use is justified only for times $t \gg T_2$. We get:

$$\begin{aligned} w(\omega, \bar{\omega}_0) &= \int_0^\infty d\omega_0 \frac{\pi\omega_0}{\hbar\epsilon L^3} |\hat{e}_\sigma \cdot \mu|^2 n_\sigma \delta(\omega - \omega_0) \frac{1}{\pi T_2} \\ &\quad \times \frac{1}{(\omega_0 - \bar{\omega}_0)^2 + (1/T_2)^2} \\ &= \frac{\omega n_\sigma}{\hbar\epsilon L^3} |\hat{e}_\sigma \cdot \mu|^2 \frac{T_2}{T_2^2(\omega - \bar{\omega}_0)^2 + 1} . \end{aligned} \tag{8}$$

Here ϵ is the permittivity of the medium. We note that in Ref. 31 it was assumed that $\omega = \bar{\omega}_0$. Also note that we use m.k.s. units.

The total average field energy density is equal to:

$$\tfrac{1}{2}\epsilon E_0^2 = \frac{\hbar\omega n_g}{L^3}\,, \tag{9}$$

where we have taken for the electric component of the radiation field (in the medium):

$$\mathbf{E}(t) = \mathbf{E}_0 \cos\omega t\,. \tag{10}$$

E_0 is the absolute value of $\mathbf{E}_0$. Substitution of Eq. (9) into (8) gives finally

$$w(\omega, \bar{\omega}_0) = \frac{T_2}{2}\left(\frac{\mu_{12}^2 E_0^2}{\hbar^2}\right)\frac{1}{T_2^2(\omega - \bar{\omega}_0)^2 + 1}\,, \tag{11}$$

where μ_{12} is the value of the component along $\mathbf{E}_0$ of μ. This is the induced transition rate formula, that will be used in the calculations simulating the experimental transients. It accounts for what we usually call off-resonance pumping, meaning that excitation of the transition is possible in the wings of the homogeneous line ($\omega \neq \bar{\omega}_0$). Note here that on-resonance ($\omega = \bar{\omega}_0$) w is proportional to T_2: as a result of taking the normalized Lorentzian line shape, a greater homogeneous width (shorter T_2) should lead to a lower on-resonance transition rate (considering the case where μ_{12} remains constant).

Because of the off-resonance pumping and the inhomogeneous broadening of the transition, the result, obtained by inserting Eq. (11) into Eq. (4), has to be convoluted with the inhomogeneous line shape $g(\bar{\omega}_0, \omega_c)$ (which can be taken Gaussian in our case, see Sec. IV A). Here ω_c is the inhomogeneous line center. As in Eq. (4) the roots s_1 and s_2 as well as the coefficients c_0, c_1, and c_2 all depend on w, this integration over $\bar{\omega}_0$ will be carried out numerically.

Now with the final result

$$N_2(\omega, \omega_c, t) = \int_0^\infty g(\bar{\omega}_0, \omega_c) N_2[(\omega - \bar{\omega}_0), t]\, d\bar{\omega}_0\,, \tag{12}$$

one should be able to explain the experimental fluorescence transients, as in each experiment the emission in a *total* vibronic line was detected (Sec. II A).

C. Related theories

We want to discuss the limitations of the theory given above in relation with a more general treatment in terms of elements of the density matrix. As was pointed out before, on a timescale $t \sim T_2$ it is incorrect to apply the theory using the w Formula (11). Then the dephasing has to be considered explicitly and a density matrix treatment is necessary, where the dephasing time T_2 and the off-resonance pumping appear in the equations of motion for the off-diagonal elements. When solving, in this formalism, the set of differential equations using the Laplace transform technique, the roots have to be found of an equation of a degree two higher than was the case in the kinetic approach. When, for example, all three $|3i\rangle$ levels are taken into account (Appendix A), an equation of degree four appears in the kinetic approach. In this case the density matrix treatment yields an equation of degree six, which has to be solved numerically.

In explaining our experiments, where the time region of interest $t \gg T_2$, we prefer to use the population kinetic approach, because of the lower degree of the equation appearing in the Laplace transformation procedure. As a consequence, however, our theory cannot be used to study the initial peak at the onset of our fluorescence transient signal.

The population flow in the same level system as that of Fig. 2 is also considered in another type of experiment. Here, fluorescence transients appear upon radiating microwave power into one or two of the transitions between the triplet spin-sublevels $|3i\rangle$: optically detected magnetic resonance (ODMR) at zero field (see, for example, Refs. 32 and 33). Kinetic theories have been developed[32,33] for the level scheme of Fig. 2, using several limiting conditions, which are not valid in the experiments described in this paper. Using transient ODMR spectroscopy one can determine for the individual $|3i\rangle$ sublevels the total decay rates (radiative plus radiationless) and the relative populating probabilities. Inserting these values in our theory (Sec. III B and Appendix A), one can determine the *absolute* $|3i\rangle$ populating rates by performing the kind of experiment described in this paper. Of course, a combination of ODMR experiments and accurate quantum yield measurements will also give these absolute populating rates.[34]

D. The effect of intermediate triplet states

It is important to consider in some detail the possibility of a second electronic triplet state (T_2^*) lying below the lowest excited singlet state S_1. Neither the experiments described in this paper nor the ODMR experiments mentioned above can, in general, discriminate between the situations where the state T_2^* lies above or below S_1.[35] However, indications about the position of T_2^* relative to S_1 might be provided by a study of the low field Zeeman effect on ODMR.[36] Such indications can also be obtained for pentacene in p-terphenyl, using the fluorescence transients, as shown in Sec. V C.

A few remarks have to be made concerning the effect of T_2^* lying below S_1 on our theoretical results. In the beginning of this section it was argued that such a T_2^* level could be left out of consideration in the kinetic treatment because of fast internal conversion to the lowest triplet state T_1. Therefore, when our theory is applied to such an electronic level structure, $S_0 \leftarrow T_2^*$ ISC is ignored, and in principle the obtained ISC rate k_{23} is the *effective* crossing rate for $T_1 \leftarrow S_1$. If the decay rate of such a T_2^* state were comparable to the other rates in the system, the $T_2^{*x,y,z}$ manifold should be explicitly included in the theory.

Note here that concerning the T_2^* level, the same approximations underlie our OFID theory.[24]

E. Applicability of the theory

We now will discuss a few properties of the excitation pulses used in the AOM experiments, to verify if the experimental conditions justify the use of the kinetic theory.

First consider the pulse risetime (30 ns). It falls in

TABLE II. Summary of the results of experiments and computer simulations for the lower sites (proto and perdeutero). λ_{det} denotes the detection wavelength. The last two columns give the $|3\rangle \leftarrow |2\rangle$ intersystem crossing yield and the $|1\rangle \leftarrow |3\rangle$ intersystem crossing rate k_{31}, both obtained by simulating the experimental signals. The error in the experimental values of τ is ± 0.5 μs and in those of $I10/I80 \pm 0.03$. Note that the simulations have been performed, assuming that only one $|3i\rangle$ sublevel is populated (see the text). For each site the signals were simulated for each power and the average values of the results are given in the last two columns. For values of these parameters lying within the error regions given, we find theoretical values for τ and $I10/I80$, lying within their experimental error limits.

		Experimental			Calculated	
site	λ_{det} (Å)	$\tau(\mu s)$	$I10/I80$	laser power (relative)	$\|3\rangle \leftarrow \|2\rangle$ yield (%)	$k_{31}(10^4\ s^{-1})$
		19.7	1.40	1		
O_1 proto	6365	17.1	1.48	2	0.47 ± 0.10	2.2 ± 0.1
		15.8	1.52	2.5		
	6365	20.6	1.29	1		
		19.3	1.42	2		
O_2 proto	6449	21.6	1.34	1	0.38 ± 0.10	2.2 ± 0.1
		19.5	1.40	2		
		18.7	1.48	2.9		
		22.7	1.65	1		
O_2 deutero	6435	21.4	1.74	2	0.50 ± 0.05	1.3 ± 0.2
		21.3	1.78	2.8		

the region of time where the use of the theory, developed in Sec. III B, is not justified. As we are interested in the time domain where this *is* justified, we are only concerned with the constant intensity value the pulse reaches after about 40 ns.

Next we are concerned with the effective bandwidth of the exciting light, in connection with the use of Eq. (7) in deriving the final formula for the induced transition rate w. Here we have to take into account two bandwidth effects. First, for a period of time of 80 μs (excitation pulse width) the frequency jitter of the dye laser will cover a bandwidth of the order of 100 kHz.[37,38] As this is very much smaller than the homogeneous width of the pentacene $|2\rangle \leftarrow |1\rangle$ transition, the assumption in Sec. III B of the exciting radiation to be perfectly monochromatic does not seem too unrealistic.

Secondly, for the first part of the pulse, we have to consider a frequency width $\Delta\omega$ in the molecule–field interaction which is related, by the uncertainty principle, to the short period of time Δt, that has elapsed since the onset of this interaction. The earliest point used in the computer fitting to the observed fluorescence transients, is $t = 0.5$ μs (theoretically the pulse was taken rectangular, starting at $t = 0$). For $\Delta t = 0.5$ μs we get, using $2\pi\,\Delta\nu\,\Delta t = \Delta\omega\,\Delta t \sim 1$, $\Delta\nu \sim 0.3$ MHz. Thus already for the first time "point" considered in the calculations, this uncertainty width is much smaller than the homogeneous width of the transition studied, which in turn is very much smaller than the inhomogeneous width. Therefore, as already stated in Sec. III B, we assume the long time limit formula (7) to hold in the time region of interest in our experiments.

We finally wish to note here a consequence of using a three-level system in simulating the experimental transients. In this way we will for the total ISC rate from S_1 (k_{23}) obtain a value very close to the real one. However, the obtained k_{31} value is not directly related to k_{31}^x, k_{31}^y, and k_{31}^z.

F. Calculation of the induced transition rate

We will now calculate the induced transition rate, that has to be used to fit the experimental fluorescence transients. From Eq. (11), we have, on resonance:

$$w_{max} = \frac{T_2}{2}\left(\frac{\mu_{12}E_0}{\hbar}\right)^2 = \frac{T_2}{2}\left(\frac{\mu E_\mu}{\hbar}\right)^2 , \tag{13}$$

where $\mu = |\boldsymbol{\mu}|$ and E_μ is the absolute value of the component of $\mathbf{E}_0$ along $\boldsymbol{\mu}$. A relative laser power of 2.5 (Table II) corresponds to 5.75 mW on the crystal, taking into account the transmission of L_1 and of the Dewar windows. The beam waist at the crystal has a diameter of 100 ± 30 μ. One obtains for a 100 μ diameter an intensity I at the crystal of 7.3×10^5 W/m^2. Of this intensity no more than a few percent is scattered by the crystal. Note that this power density is about a factor of 10^3 higher than that used in the OFID experiments reported earlier.[1,24] The pentacene $S_1 \leftarrow S_0$ transition dipole moment $\boldsymbol{\mu}$ is aligned along the short molecule axis.[23] As this is parallel to the p-terphenyl short axis,[39] and the angle between this axis and the crystal b axis is 34°,[40,41] the angle between $\boldsymbol{\mu}$ and the polarization direction of the laser is 34°. Furthermore it was calculated that $E_b^{loc} = 1.78\,E_b^{ext}$,[42] relating the values along the b-axis of the local field $\mathbf{E}^{loc}$ and the field $\mathbf{E}_0^{ext}$ just in front of the crystal. We now take

$$E_\mu^{loc} = 1.78\,E_b^{ext}\cos 34^\circ . \tag{14}$$

Using the relation

$$(E_b^{ext})^2 = \frac{2I}{v_{He}\epsilon_{He}} , \tag{15}$$

where v_{He} and ϵ_{He} are the velocity of light and the value of the permittivity in liquid helium at 2 K, respectively,

TABLE III. For the different sites (p) and (d) denote proto and perdeutero, respectively. The figures in the table without further reference were measured or calculated in this work. τ_{fl} is the fluorescence $1/e$ lifetime. The values given for w_{max} correspond to a relative laser power of 1 (Tables II and IV), and are calculated as discussed in Sec. III. F. $\Delta\omega_G$ is 2π times the measured FWHM of the respective absorption line. The values of the absorption and $\Delta\omega_G$ were determined, using the same crystal as that used in the fluorescence–transient measurements. The given absorption values are those at the inhomogeneous line centers.

Site	O_1(p)	O_2(p)	O_2(d)	O_3(p)	O_3(d)	O_4(p)	O_4(d)
τ_{fl}(ns)	23.5[a]	23.5[a]	27.5[a]	9.5±1.5	11.6±1.5	10.0±1.5	15.6±1.5
T_2 (ns) (at 2 K)	45[a,b]	45[a,b]	54[a,b]	19[c]	23.2[c]	20.0[c]	31.2[c]
w_{max} (10^9 s^{-1})	5.2	5.2	6.2	2.2	2.7	2.3	3.5
Absorption (%)	17.0	18.5	5.4	19.6	5.9	16.4	4.9
$\Delta\omega_G/2\pi$ (GHz)	21	24	30	24	23	21	24

[a]Reference 7. [b]Reference 1. [c]Here T_2 was taken to be equal to $2\tau_{fl}$.[21]

we finally obtain $E_\mu^2 = 1.2\times10^9$ V^2/m^2 (the superscript loc in E_μ has been dropped), corresponding to a relative laser power of 2.5. At a certain power, w_{max} will be different for the different pentacene sites, as it depends on T_2 and μ, according to Eq. (13). Note once again, that our experiments were performed at 2 K, where for the system under study $T_2 = 2\tau_{fl}$.[1,7,21] For the O_1 site (proto), for example, the relative power of 2.5 corresponds to $w_{max} = 1.3\times10^{10}$ s^{-1}, as $T_2 = 45$ ns[1,7] and $\mu = 0.71$ D (see below). The calculated values for w_{max} (for relative laser power 1) can be found in Table III.

Note that the obtained value for w_{max} does not depend on the specific local field approximation. The extrapolation of τ_{OFID} to zero laser power[24] yields the product of μ and a local field correction factor. When in the calculation of μ from this product as well as in the calculation of w_{max} from this μ the same local field correction is applied, w_{max} becomes independent of this correction.

G. The computer simulations of the fluorescence transients

We will now discuss the computer simulation of the fluorescence transients. We start with a choice for the values of the ISC rates k_{23} and k_{31}. Consider a certain time t. For this time we have to perform the inhomogeneous integration of Eq. (12). From (11), we have for the induced transition rate

$$w = \frac{w_{max}}{T_2^2\Delta^2 + 1}, \tag{16}$$

where w_{max} is defined in (13) and $\Delta \equiv \omega - \bar{\omega}_0$. The values of w_{max} and T_2 for the different pentacene sites are given in Table III. As a detuning parameter we choose the dimensionless product $T_2\Delta$, and let its value increase according to 0, 1, 2, 3 . . . , etc. The Gaussian (Sec. IV A) inhomogeneous lineshape has to be taken into account:

$$N_0 = N_0^c \exp\left[-\left(\frac{2\sqrt{\ln 2}(\bar{\omega}_0 - \omega_c)}{\Delta\omega_G}\right)^2\right], \tag{17}$$

where N_0^c is the number of molecules at the top of the absorption line, ω_c is the inhomogeneous line center and $\Delta\omega_G$ is the FWHM of the inhomogeneous absorption line. The values of $\Delta\omega_G$ for the different sites are given in Table III. As in every experiment the laser frequency was tuned to the top of the absorption line, we have $\omega = \omega_c$ and

$$N_0 = N_0^c \exp\left[-\left(\frac{2\sqrt{\ln 2}T_2\Delta}{\Delta\omega_G \cdot T_2}\right)^2\right]. \tag{18}$$

For a certain value of $T_2\Delta$ then, using the method of calculation of Sec. III B, a value is obtained for the quantity

$$\frac{N_2(t,\Delta)}{N_0^c} = \exp\left[-\left(\frac{2\sqrt{\ln 2}T_2\Delta}{\Delta\omega_G \cdot T_2}\right)^2\right] w(c_0 + c_1 e^{s_1 t} + c_2 e^{s_2 t}). \tag{19}$$

This is added to the sum of the values of this quantity, that were calculated for the values of $T_2\Delta$, run through already [compare Eq. (12)]. This numerical integration for time t is extended until $T_2\Delta = T_2\Delta_{max}$, where the value of $N_2(t, \Delta_{max})/N_0^c$ is less than 1/5000 (Sec. IV D) of the sum of the $N_2(t,\Delta)/N_0^c$ values for $T_2\Delta = 0$ through $T_2\Delta = T_2(\Delta_{max} - 1)$. This sum times 2 is equal to $N_2(\omega = \omega_c, t)/N_0^c$ [compare Eq. (12)]. This calculation was carried out for $t = 0.5$ μs through $t = 80$ μs (0.5 μs increments). Then the $[N_2(\omega, t)/N_0^c, t]$ curve, to be compared with the experimental fluorescence transient, is obtained. In Figs. 4 and 5 the best computer fits are denoted by small circles, and are obtained by consecutively improved choices for k_{23} and k_{31}.

Also a calculation was made with the laser frequency placed in the wing of the inhomogeneous absorption line $[(1/2\pi)|\omega - \omega_c| = 23$ GHz], for the O_2 site (proto). Compared with the $\omega = \omega_c$ case, τ and $I10/I80$ were found to be identical. It thus follows from our theory, that for the fluorescence–transient measurements the precise excitation frequency relative to ω_c is not important. This was not verified experimentally. Observations, reported by Orlowski *et al.*[8] seem to contradict this theoretical result. A careful experimental study, where the occurrence of energy transfer is excluded, might provide a solution on this point.

IV. RESULTS

A. Lower site (O_1,O_2) results

The nomenclature of the sites is given in Fig. 3, showing the absorption spectrum of pentacene-h_{14} in p-

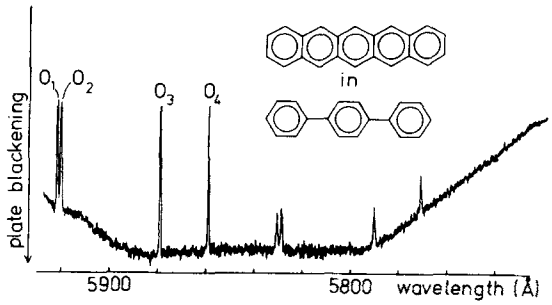

FIG. 3. Absorption spectrum of pentacene-h_{14} in p-terphenyl at 2 K.[43] A densitometer trace is shown of the photographic plate. O_1 through O_4 denote the origins of the four different sites that are occupied by the pentacene molecules in this host crystal. For all the sites the first vibronic transition is also shown.

terphenyl. This spectrum was obtained several years ago in our laboratory.[43]

Typical fluorescence transient signals obtained from the lower sites, using the experimental set-up of Fig. 1, are depicted in Fig. 4. It turns out that the time dependence of the transient b part is purely exponential. We will characterize these signals by two parameters: the $1/e$ decay time of the b part (τ) and the ratio of the total signal intensities at 10 and 80 μs ($I10/I80$). It follows from Sec. III B that the initial peak intensity is not a useful parameter to be compared with our theory.

The experimental results, obtained from the lower sites, are gathered in Table II. For perdeuteropentacene, measurements were done only on the O_2 site, as the O_1 site overlaps with partially deuterated pentacenes of the O_2 site.[7] For the O_2 site (proto) the experiment was done using the fluorescence of two different vibronic

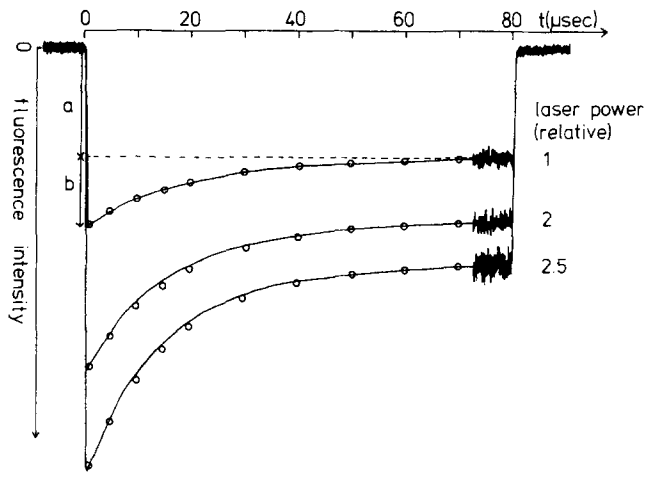

FIG. 4. Transient fluorescence of pentacene-h_{14} in p-terphenyl (O_1 site) at 2 K. For clarity, the real experimental noise is only indicated in the last part of the transients. The solid lines are hand-drawn averages through the noisy experimental curves The centers of the circles are points, obtained from computer fits with τ and $I10/I80$ values within their respective experimental error regions. For one curve the constant part (signal intensity at 80 μs) is denoted by a, while b gives the transient part. The relative laser power of 1 corresponds to an intensity on the crystal of 2.9×10^5 W/m^2.

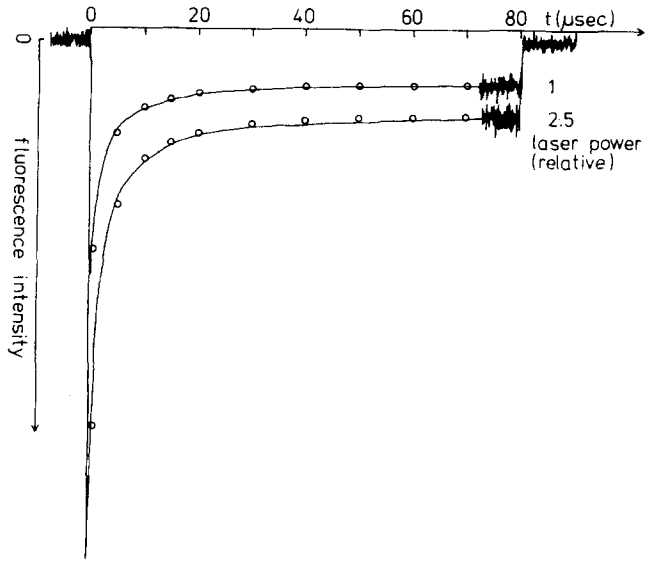

FIG. 5. Transient fluorescence of pentacene in p-terphenyl (O_3 site, proto) at 2 K. The experimental noise is only indicated in the last part of the transients. The solid lines are hand-drawn averages through the noisy experimental curves. The centers of the circles are points, obtained from computer fits giving $I2/I80$, $I10/I80$, and $I20/I80$ values within their respective experimental error regions. A relative laser power of 1 corresponds to an intensity on the crystal of 2.9×10^5 W/m^2.

lines. The results were identical within experimental error, as shown in the table.

A few observations were made of the resonantly scattered laser light, as mentioned in Sec. II A. An example of such an observation was already given in Ref. 1, Fig. 2(b), and the signal was explained as being due to the ground state becoming partly depleted in the pumping cycle (this signal should not be confused with the resonance Raman scattered light!). For this signal a transient and a constant part can be defined in a way similar to that in Fig. 4. In the resonant case, however, the transient part *increases* from the onset of the signal to later times. For the crystals used in the experiments, described in this paper, the ratio of this transient part of the signal intensity to the constant part was much smaller than in the case of Ref. 1, Fig. 2(b). The transient part originates from resonant scattering from inside the crystal and it will have a different intensity in different directions, due to macroscopic crystal irregularities. Although the resonant scattering signal was important for the interpretation of the results reported in Ref. 1, Fig. 2(a) (Fig. 4, this work), it has not been incorporated in the present analysis, as it does not seem to be of quantitative use here.

We will now briefly comment on the results of the fluorescence-transient simulations for the lower sites, which can be found in Table II. First note, that the values obtained for the $|3\rangle \leftarrow |2\rangle$ ISC yield, are extremely low. For the O_1 site (proto), for instance, this yield is 0.47%, in other words $k_{23}=2.0\times10^5$ s^{-1}. Thus $1/k_{23}=5.0$ μs. Furthermore, for the O_1 site (proto) we obtained $k_{31}=2.2\times10^4$ sec^{-1}, or $1/k_{31}=45.5$ μs. So, for example, for the O_1 site (proto), the decay time τ of the

TABLE IV. Summary of the experimental results for the higher sites. λ_{det} denotes the detection wavelength.

Site	λ_{det}(Å)	$I2/I80$	$I10/I80$	$I20/I80$	Laser power (relative)
O_3 proto	6401	3.30±0.21	1.62±0.13	1.26±0.11	1
		3.48±0.14	1.59±0.09	1.25±0.08	2
		3.43±0.13	1.66±0.06	1.29±0.06	2.5
O_3 deutero	6385	4.38±0.43	1.88±0.30	1.44±0.25	1
		4.00±0.33	1.83±0.19	1.43±0.16	2.1
		4.18±0.27	1.92±0.15	1.47±0.13	2.7
O_4 proto	6376	3.15±0.35	1.59±0.22	1.27±0.19	1
		3.21±0.19	1.55±0.12	1.21±0.10	2.6
O_4 deutero	6361	4.07±0.47	1.92±0.27	1.47±0.22	1
		3.58±0.22	1.76±0.12	1.42±0.10	2.7

fluorescence transients (19.7 μsec for a relative power of 1) is clearly determined by *both* the $|3\rangle \leftarrow |2\rangle$ and the $|1\rangle \leftarrow |3\rangle$ ISC processes. The obtained k_{31} values are in reasonable agreement with the preliminary data of Weissman and Kim.[28] They are also consistent with the triplet decay rates in the gas phase ($3\times10^4\,s^{-1}$ [44]) and in benzene solutions at 50 °C ($1.4\times10^4\,s^{-1}$ [45]), both measured by triplet–triplet absorption. A more extensive discussion of the results is given in Sec. V.

Now a few remarks will be made concerning the absorption spectra of the origins of the several proto and perdeutero pentacene sites. The absorption and FWHM values are given in Table III. The line shapes were also examined. Some of the lines exhibited a slight asymmetry, but at least one wing of all the lines had a perfect Gaussian shape. This shape was used in the fluorescence-transient simulations. This turned out to be a correct assumption, as the region that was effectively off-resonance pumped, was in all cases less than 3 GHz to each side of the inhomogeneous line center (in each experiment the excitation frequency was adjusted so, that $\omega = \omega_c$).

The fluorescence lifetime (τ_{f1}) of the O_1 site (proto) was measured in the temperature range 39–110 K as described in Sec. II B. It was constant in this range and equal to 22±1 ns, which is, within experimental error, equal to the low temperature (2 K) value.[7] The measurements were not continued to higher temperatures, as the signal to noise ratio decreased with increasing temperature.

The k_{23} and k_{31} values obtained here, were just the data, needed to calculate the $S_1 \leftarrow S_0$ transition dipole moment from our earlier OFID experiments.[1] This calculation,[24] yields finally for the O_1 site (proto) $\mu = 0.71 \pm 0.24$ D. Note that we deal here with a parameter variation cycle. The value of μ was needed to calculate the power, used in the fluorescence-transient experiments, while the results of the fluorescence-transient simulations are used to calculate μ. However, the lower site k_{23} and k_{31} values obtained from the simulations, are very insensitive to power variations, leading to unambiguous results for k_{23}, k_{31}, and μ. In the w_{max} calculations (Table III), μ was assumed to be identical for the higher and the lower pentacene sites. Since μ for perdeuteropentacene does not differ significantly from the proto value[1] and as the lower site k_{23} and k_{31} results are very power insensitive, we took also $\mu = 0.71$ D in calculating w_{max} for the perdeutero sites (Table III).

As the fluorescence transient and the OFID experiments provided us with a value for μ, it is possible to calculate the absolute pentacene concentration in the sample crystal, using the data from the absorption spectrum. This is shown in Appendix B.

B. Higher site (O_3,O_4) results

Typical higher site fluorescence transient signals also obtained with the experimental set-up of Fig. 1, are shown in Fig. 5. As no exponential behavior is recognizable in these transients, they will be characterized by the following 3 parameters: $I2/I80$, $I10/I80$, and $I20/I80$. These are the signal intensities at 2, 10, and 20 μs, respectively, all divided by the intensity at 80 μs.

The experimental results for the higher sites are given in Table IV.

The fluorescence lifetimes of the higher sites were also measured at 2 K, as described in Sec. II B. The results were obtained from photographs of the oscilloscope trace and are given in Table III.

It is *a priori* not clear which one of the two radiationless decay channels from S_1 causes the drop in fluorescence lifetimes for the higher sites compared to the lower ones. Despite the increase in the $S_1 - S_0$ energy separation of only about 150 cm^{-1}, a significant contribution of $S_0 \leftarrow S_1$ internal conversion to the fluorescence lifetime drop cannot be excluded. In order to simulate the higher site fluorescence transients, it seemed reasonable to us to start with the assumption that the T_1 depletion rate k_{31} has identical values for the lower and higher sites (T_1 is expected to undergo an energy shift which is much smaller than that of S_1, upon going from the lower to the higher sites[46]). Maintaining k_{31} within the error regions obtained for the lower sites, the simulations of the higher site fluorescence transients give, for example, for the O_3 site (proto) the result that 10% $\lesssim |3\rangle \leftarrow |2\rangle$ yield $\lesssim$60%. The large uncertainty in the obtained $|3\rangle \leftarrow |2\rangle$ >ISC yield can be easily explained, as

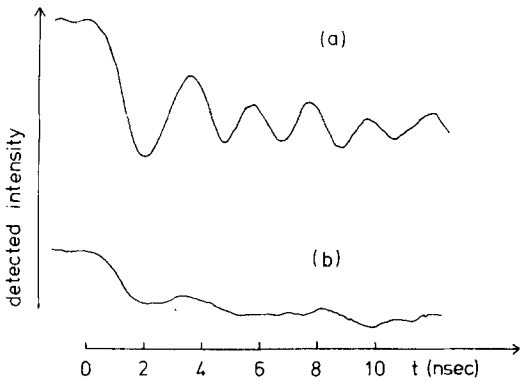

FIG. 6. OFID signals from pentacene in p-terphenyl at 2 K, obtained by extracavity laser-frequency switching (~500 MHz switch), (a) for the O_1 site (proto) and (b) for the O_3 site (proto) In both cases the laser intensity (unfocused) upon the crystal was 1.5 mW/mm^2.

the 10 and 60% values correspond to $1/k_{23}=95$ and 16 ns, respectively. Thus only during about the first 100 nsec the signal will be very sensitive for the precise value of k_{23}, while the first time "point" considered in the simulations was $t=2$ μs. An accurate value for the k_{23} ISC rate may be obtained from this kind of experiment by using (a) an AOM with a shorter rise time and (b) a density matrix theoretical treatment. See also Sec. IV C.

C. OFID

Also in OFID the higher sites show a behavior, markedly different from that of the lower sites. This is shown in Fig. 6. This result is a beautiful illustration of the OFID theory, given in Ref. 24, and indicates a large increase in $|3\rangle \leftarrow |2\rangle$ ISC yield. From the OFID signal of Fig. 6(b) we will make an estimate of this yield for the O_3 site (proto). From our experience with OFID we conclude, that for a certain OFID signal with $1/e$ decay time τ_{OFID}, no recognizable beat signal exists after a time of about $3.5\,\tau_{\mathrm{OFID}}$. As we consider the signal of Fig. 6(b) to exhibit just the onset of an OFID beat pattern, we conclude that $\tau_{\mathrm{OFID}}=1\pm0.15$ ns. Then from Eq. (18) of Ref. 24 for $1/\tau_{\mathrm{OFID}}$, one calculated $A\sim3000$. For the three-level model considered in this work, we have $A=k_{23}/k_{31}$. The final result is: $|3\rangle \leftarrow |2\rangle$ ISC yield $\lesssim 60\%$, where the k_{31} result of the present work is used. It was assumed here, that at 2 K also for the higher sites $T_2=2\tau_{f1}$. Although the uncertainty in the obtained ISC value is quite large, it indicates a drastic increase in the $|3\rangle \leftarrow |2\rangle$ ISC yield compared to the lower sites.

We note here that it might be worthwhile to perform OFID experiments on the O_3, O_4 sites employing a much faster frequency switch.[47] Such an experiment would unambiguously settle the question whether the drop in fluorescence lifetime is exclusively due to an increase in intersystem crossing.

We finally want to exclude the possible role of intersite communication in the shortening of τ_{f1} of the higher sites compared to the lower ones. Upon excitation in the higher site origins no emission from the lower sites was observed. Also energy transfer within the pentacene inhomogeneous line[7] does not take place in the experiments described in the present paper: our lower site OFID experiments, reported in Ref. 1, were performed on the same crystal as that used in the presently described experiments and a T_2 was obtained, which was completely determined by the fluorescence lifetime.

It is interesting to make a comparison with the behavior in OFID of pentacene -h_{14} in naphthalene. Here the pentacene $S_1 \leftarrow S_0$ transition is lying 302 cm^{-1} lower in energy (0–0 at 6028 Å[48]) than for the lower sites in p-terphenyl, and $\tau_{f1}=20$ ns.[49] For the 6028 Å transition, the observability of OFID at 2 K using intracavity laser frequency switching[1,5,50] was comparable[51] to that from the lower sites in p-terphenyl.[1] With an intensity at the crystal $I=0.26$ mW/mm^2 we measured $\tau_{\mathrm{OFID}}=7\pm1.5$ ns. We assume a pentacene molecule to replace two translationally equivalent naphthalene molecules along the c axis in the mixed crystal. As the pentacene $S_1 \leftarrow S_0$ transition moment is aligned along the short molecule axis,[23] it will be approximately parallel to the crystal b axis, which in turn was parallel to the laser polarization direction. Using for the refractive index $n_b=1.72$[52] and the Lorentz local field approximation, one obtains $E_\mu^{\mathrm{loc}}=1.65\,E_b^{\mathrm{ext}}$, whereupon the field amplitude E_μ is easily calculated [Eq. (15)]. We take μ to be equal to 0.71 ± 0.24 D, which was obtained for the lower sites in p-terphenyl, and we take $T_2=2\tau_{f1}=40$ ns (temperature 2 K). We calculate, using Eq. (18) of Ref. 24, for pentacene in naphthalene: $A<64$. In the three-level approximation, $A=k_{23}/k_{31}$. Taking for the T_1 decay rate k_{31} the value obtained above for the lower (proto) sites in p-terphenyl, we get for the $T_1 \leftarrow S_1$ ISC rate in pentacene in naphthalene: $k_{23}<1.4\times10^6$ s^{-1}, or $T_1 \leftarrow S_1$ ISC yield $<2.8\%$. With a radiative lifetime τ^R of 30 ns (see Sec. V B) we obtain a fluorescence quantum yield of 0.67, and an $S_0 \leftarrow S_1$ internal conversion yield between 0.30 and 0.33.

D. Off-resonance pumping in a three-level system

Let us consider the part of the inhomogeneous absorption line that is active in the pumping cycle. The calculations show, that if the numerical integration boundary value is made smaller than 1/5000 (Sec. III G), this has no effect on the values obtained for τ and $I10/I80$. Therefore we take $T_2\Delta_{\mathrm{max}}$, obtained with this boundary value, as a measure for that part of the inhomogeneous line that is pumped. For the O_2 site (proto), for example, for relative power we have for $t=80$ μs, $T_2\Delta_{\mathrm{max}}=2\pi T_2(\nu-\bar{\nu}_0)_{\mathrm{max}}=380$ or $(\nu-\bar{\nu}_0)_{\mathrm{max}}=(380/2)[(1/\pi T_2)]$ to one side of the inhomogeneous line center. Thus the part of the absorption line, with $\Delta\nu_G=24$ GHz, being active in the pumping cycle is 380 homogeneous widths, which amounts to 2.7 GHz.

We further would like to consider the off-resonance pumping for our three-level system in some detail. For this study $N_2(t,\Delta)/N_0$ was calculated as a function of Δ, for a limited Δ range, and for several times after the onset of the exciting pulse. For simplicity we consider here a flat inhomogeneous distribution (which for the case under study is quite realistic, as only a small central portion of the inhomogeneous line is pumped).

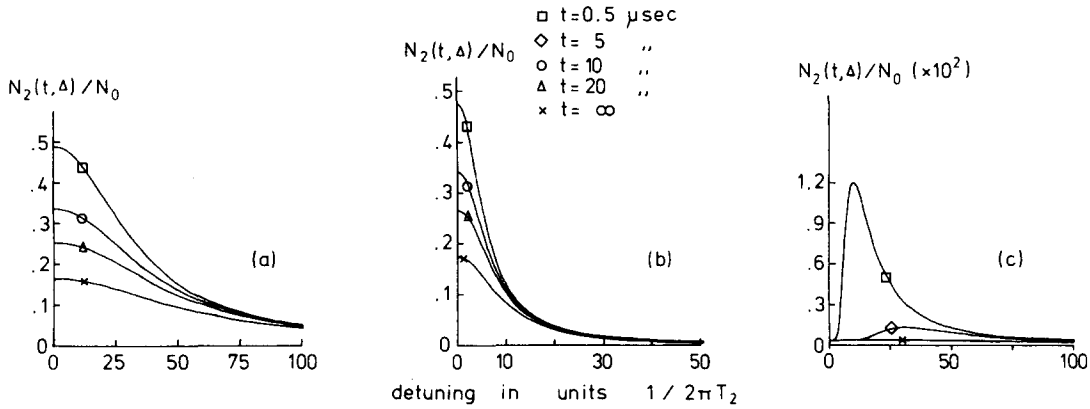

FIG. 7. Time-dependent off-resonance pumping for a three-level system. As the pumping behavior is symmetrical with respect to the excitation frequency, only one half of the curves is shown. (a) These curves were calculated with the parameter values for the O_2 site (proto). w_{max} was here 2.4×10^{10} s^{-1} and the $|3\rangle - |2\rangle$ ISC yield 0.2%. A detuning of 100 corresponds here to an off-resonance frequency of $100/2\pi T_2 = 354$ MHz. (b) Again O_2 site (proto), where now w_{max} was equal to 6.6×10^{8} s^{-1}, while the $|3\rangle \leftarrow |2\rangle$ ISC yield was 0.2%. (c) These curves were calculated with the parameter values for the O_3 site (proto). w_{max} was here 3.6×10^{8} s^{-1}, and the $|3\rangle \leftarrow |2\rangle$ ISC yield 59.7%. Note the difference in the vertical scale, compared with (a) and (b). Now a detuning of 100 corresponds to an off-resonance frequency of $100/2\pi T_2 = 838$ MHz. (See also Note added in proof. The only effect of taking into account the power broadening is that the numbers on the vertical scale of Figs. 7(a) and 7(b) should be divided by 2.)

In other words

$$\frac{N_2(t,\Delta)}{N_0} = w(c_0 + c_1 e^{s_1 t} + c_2 e^{s_2 t}), \tag{20}$$

where N_0 is now the number of molecules at every detuning value. Also

$$\frac{N_2(\infty,\Delta)}{N_0} = wc_0\,, \tag{21}$$

was calculated, which is identical to the steady-state value

$$\frac{N_2(\Delta)_{st.st.}}{N_0} = \frac{wk_{31}}{K_2 k_{31} + 2wk_{31} + wk_{23}}\,. \tag{22}$$

The results are given in Fig. 7. Consider first Fig. 7(a). As here $1/k_{23} = 11$ μs, at $t = 0.5$ μs we have (on resonance) practically a power-saturated two-level system: $N_2(0.5, 0)/N_0 \approx 0.5$. This value decreases as the time develops because of the storage of population in level $|3\rangle$. It is interesting to make a comparison here of Figs. 7(a) and 7(b) with Fig. 6.2, page 141 of Ref. 31, where the steady-state inversion of a two-level system is displayed as a function of detuning. The curves in Figs. 7(a) and 7(b) for $t = 0.5$ μs may be directly related to the curves of Fig. 6.2 of Ref. 31, as 0.5 μs $\gg T_2$, τ_{f1}, and level $|3\rangle$ has not yet become of importance (0.5 μs $\ll 1/k_{23}$). Thus the 0.5 μs curves of Figs. 7(a) and 7(b) may be considered as two-level steady-state curves. As time proceeds level $|3\rangle$ plays its part, and the curve develops to its three-level steady-state shape. Figure 7(b) just shows the effect of power reduction with a factor 36, relative to Fig. 7(a). Now consider Fig. 7(c). Here the influence of level $|3\rangle$ is very marked, as $1/k_{23} = 16$ ns. Follow, for example, the 0.5 μs curve for increasing detuning. On resonance, level $|2\rangle$ is nearly completely depleted compared to the situation of Fig. 7(b). Now almost the total population of the level system is stored in level $|3\rangle$. As Δ increases, the induced transition rate w ($|2\rangle \leftarrow |1\rangle$ and $|1\rangle \leftarrow |2\rangle$) decreases relative to k_{23}, causing an off-resonance maximum in the population N_2. As w further decreases with increasing Δ, less population is pumped from $|1\rangle$ to $|2\rangle$, and for $T_2\Delta = 100$ nearly the total population remains in the ground state $|1\rangle$.

V. DISCUSSION

A. The $|1\rangle \leftarrow |3\rangle$ ISC rate

For the moment, just consider the proto sites. The k_{31} values obtained in this work are consistent with the pentacene triplet decay rates obtained before,[28,44,45] as mentioned in Sec. IV A. The values estimated for the $T_1 - S_0$ energy separation range from 6400 to 8300 cm^{-1}.[53-57] These values and those obtained for k_{31} are consistent with what one would expect from the relation that exists between k_{31} and the T_1 energy for unsubstituted aromatic hydrocarbons (Fig. 5.1 and Table 5.3 of Ref. 27). Thus pentacene has a relatively low lying T_1 state with a high decay rate, which is completely radiationless as the radiative T_1 decay rate is expected to be about 0.03 s^{-1}.[27] Note here that the high k_{31} value is crucial to the observation of OFID from pentacene.[24] Upon deuteration, k_{31} decreases, as expected for a $S_0 \leftarrow T_1$ radiationless transition.[27]

B. The lower site $|3\rangle \leftarrow |2\rangle$ ISC rate

Now consider the very low value obtained for the ISC rate k_{23} for the lower sites (proto), being 1.7×10^{5} s^{-1} (corresponding to a $|3\rangle \leftarrow |2\rangle$ yield of 0.4%). Incidentally note that this very low k_{23} value for the lower sites is also crucial to the observation of OFID.[24] However, for most unsubstituted aromatic hydrocarbons studied, k_{23} is much larger due to a second triplet state T_2^* lying energetically lower than the S_1 state.[27] This indicates that for the lower sites of pentacene in p-terphenyl, ISC from S_1 only occurs to T_1. There are a few other examples where the ISC yield from S_1 is negligible. Here T_2^* is lying above S_1: crystalline anthracene,[58] pyrene,[59] and some substituted anthracenes.[60,61] Note that while

in both pyrene and pentacene the S_1-T_1 gap is $\sim 10\,000$ cm^{-1}, their k_{23} values are also very similar [3×10^4 s^{-1} for pyrene (p. 231 of Ref. 27)]. For pentacene some energy level calculations predict T_2^* to lie very close to S_1.[56]

Thus from a comparison with other polyacenes one may conclude that an explanation of the very low k_{23} value will somehow be related to the position of a second triplet state relative to S_1. Further discussion on this point is given below.

As the $|3\rangle \leftarrow |2\rangle$ quantum yield is negligibly small, the decay of the S_1 state occurs radiatively and by $S_0 \leftarrow S_1$ internal conversion. Using the radiative lifetime of the pentacene $S_1 \leftarrow S_0$ transition, calculated in Ref. 62 ($\tau^R = 30$ ns), it is possible to make an estimate of these two decay channels for the lower sites in p-terphenyl. For the fluorescence quantum yield one obtains $\phi_F = \tau_{f1}/\tau^R = 0.78$, in other words the internal conversion yield is 0.22. Thus in the lower sites in p-terphenyl, pentacene exhibits an appreciable $S_0 \leftarrow S_1$ internal conversion, as it does in solution[62] and in the gas phase.[44] Note that also in the case of pentacene in naphthalene this internal conversion yield is considerable (Sec. IV C). It is one of the few polyacenes, where this process is of importance.[27,63]

As a last point concerning the lower sites, note the absence of a sizeable deuteration effect on the k_{23} rate. This is another indication that in the lower sites ISC from S_1 occurs to T_1.[27] However, it should be noted here that this does not exclude T_2^* lying below S_1, when the $T_2^* - S_1$ gap is small ($\lesssim 1000$ cm^{-1}).[64,65]

C. The higher site $|3\rangle \leftarrow |2\rangle$ ISC rate

As already mentioned in Sec. IV B, a cause of the drop in fluorescence lifetime for the higher sites relative to the lower ones may be an increase in the $S_0 \leftarrow S_1$ internal conversion, despite the increase in the S_1-S_0 energy separation of only about 150 cm^{-1}, compared to the total S_1-S_0 gap of about 17 000 cm^{-1}. This is suggested by the following observations. First consider pentacene in solution at room temperature. Here $\tau_{f1} = 8$ ns,[44] the S_1-S_0 separation is 17 300 cm^{-1} (in benzene),[45] and the $S_0 \leftarrow S_1$ internal conversion yield may be as high as 0.76 (in 1-Cl-naphthalene[62]). Then consider pentacene in naphthalene at 2 K (Sec. IV C). In this case the $S_0 \leftarrow S_1$ 0–0 transition lies at 16 585 cm^{-1}, which is 302 cm^{-1} below this transition in pentacene in p-terphenyl (O_2 site, proto), and the $S_0 \leftarrow S_1$ internal conversion yield is estimated to be about 50% higher in the naphthalene host (Sec. IV C). Thus relatively small changes in the electronic energy gap may cause considerable changes in the $S_0 \leftarrow S_1$ internal conversion rate.

From the fluorescence-transient simulations (Sec. IV B) and even more strongly from the OFID result of the O_3 site (proto) (Sec. IV C) it follows that at least an important contribution to the shortening of the fluorescence lifetime upon going from the lower to the higher sites comes from an increase in the ISC rate from S_1. The large increase in k_{23} for the higher sites relative to the lower ones reminds one of a similar change in anthracene upon going from the crystal to a solution,[58] although in that case the shift of the S_1 level was about 10 times larger. The reason for the change in the anthracene ISC rate was shown to be an S_1, T_2^* level inversion. One therefore might expect that also in our case the T_2^* state plays an important role, which is moreover suggested by energy level calculations,[56] as already mentioned. In any case we conclude that for the higher sites T_2^* lies below S_1. Note here that a situation like that of pentacene in p-terphenyl is encountered for anthracene-d_{10} in n-heptane at low temperature,[66] where also different sites show different radiationless decay behavior.

If we were to encounter a similar level inversion, T_2^* would necessarily lie *above* S_1 for the lower sites. Therefore we measured τ_{f1} of the O_1 site (proto) as a function of temperature. In this kind of experiment, at high enough temperatures, thermally activated ISC can take place from S_1 to a higher T_2^* state.[27] Temperature dependent studies of τ_{f1} have, for instance, been performed for naphthalene,[67] anthracene and its derivatives,[60,61,68–70] anthracene-d_{10},[66] pyrene,[59] and other compounds.[71] Our experiment showed τ_{f1} for the O_1 site (proto) to be independent of temperature in the range 2–110 K. We conclude that for the lower sites the T_2^* state probably lies below S_1. This is consistent with the conclusion reached in Ref. 45, that the $T_2^*-T_1$ energy gap is less than 9000 cm^{-1}. Thus for the higher sites no level inversion of the type encountered in anthracene has occurred.

For a T_2^* state lying closely below S_1 (less than about 1000 cm^{-1}), the $T_2^* \leftarrow S_1$ ISC rate was shown to possibly be critically dependent on the $T_2^*-S_1$ energy separation.[64,65] When for the lower sites T_2^* indeed also lies below S_1, pentacene in p-terphenyl shows such a behavior.

We close this section by noting that the drop in fluorescence lifetime for the higher sites relative to the lower ones may well be due to increasing rates in both radiationless decay channels.

VI. CONCLUSIONS

In the first place it is now firmly established that the fluorescence transient for the lower pentacene sites in p-terphenyl is caused by the participation of the T_1 state in the optical pumping cycle, in agreement with a previous conclusion.[1] The influence of the triplet state on the fluorescence transient was quantitatively determined and the effect of the bottleneck on the OFID[24] was also experimentally demonstrated (Fig. 6). In Appendix B it is briefly shown that also in the interpretation of an ordinary $S_1 \leftarrow S_0$ absorption experiment the intermediate T_1 state has to be considered.

OFID measurements were further demonstrated to be very fruitful in combination with the fluorescence-transient experiments. This combination of experiments yields the $T_1 \leftarrow S_1$ and $S_0 \leftarrow T_1$ ISC rates as well as the S_0-S_1 transition dipole moment. For μ we obtained, finally, 0.71 ± 0.24 D [O_1 site (proto)].

It was further shown that the part of the inhomogeneously broadened absorption line that was pumped by

the cw dye laser (effective excitation bandwidth <1 MHz) had a width of a few GHz. The off-resonance pumping effect treated by Allen and Eberly[31] for a two-level system, was studied in this paper for a three-level system. It was also shown that the third level can cause an on-resonance "hole" in the population of the S_1 level [Fig. 7(c)].

From the fluorescence transients for the lower sites of pentacene (proto and perdeutero) in p-terphenyl values were obtained for the $S_0 \leftarrow T_1$ ISC rate (2.2×10^4 s^{-1} (proto)) and the $T_1 \leftarrow S_1$ ISC yield [0.47 ± 0.10% (O_1 proto)]. Using the radiative lifetime, an $S_0 \leftarrow S_1$ internal conversion yield of 22% was calculated.

For pentacene in naphthalene at 2 K the $T_1 \leftarrow S_1$ ISC and the $S_0 \leftarrow S_1$ internal conversion yields were estimated to be <2.8% and 31.5 ± 1.5% resepctively.

As in the other polyacenes studied,[27,72] for pentacene in p-terphenyl (all sites) the T_2^* state probably lies below S_1. If so, the obtained k_{23} values are the effective ISC rates.

The experiments described in this paper, combined with the theory developed in Sec. III B and Appendix A, can be used to determine the absolute values of the (effective) $|3i\rangle$ populating rates $k_{23}^{x,y,z}$, provided that the populating probabilities and decay rates are known (from ODMR experiments). Thus the (effective) $T_1 \leftarrow S_1$ ISC rate is obtained without the need of accurate quantum yield measurements. The method described here is especially useful in determining very small ISC quantum yields. For high $T_1 \leftarrow S_1$ yields, the time region $t \sim T_2$ of the fluorescence-transients will contain important information and a full density matrix treatment will become necessary.

From the mutual comparison of pentacene in p-terphenyl, in naphthalene and in liquid solution it follows that relatively small changes in electronic energy gaps may not only cause considerable changes in ISC rates (T_2^* close to S_1), but also in internal conversion rates. Thus despite the electronic energy gap being large, the radiationless transitions may occur by specific, energy-dependent, mechanisms. Similar behavior is found for the anthracene-d_{10} sites in n-heptane.[66] Recent work on vibrational relaxation in the S_1 states of pentacene in naphthalene[73] and porphin in n-octane[74] also seems to imply that the intramolecular level structure is crucial in determining the internal conversion.

We finally note that the occurrence of different sites in mixed crystals is shown to form a useful natural probe to study the energy dependence of the radiationless decay processes.

APPENDIX A. FIVE-LEVEL KINETICS

We will now discuss the kinetics of the five-level system of Fig. 2, thereby extending the three-level treatment of Di Bartolo[22] (Sec. III B). The equations of motion now become:

$$N_1 + N_2 + \sum_i N_3^i = N_0 , \tag{A1}$$

$$\dot{N}_2 = -\left(k_{21} + \sum_i k_{23}^i\right) N_2 + w(N_1 - N_2) , \tag{A2}$$

$$\dot{N}_3^i = k_{23}^i N_2 - k_{31}^i N_3^i . \tag{A3}$$

Using the initial conditions $N_1(0) = N_3^i(0) = 0$, we get for the Laplace transform $n_2(s)$ of $N_2(t)$:

$$n_2(s) = \frac{wN_0}{s} \frac{(k_{31}^x + s)(k_{31}^y + s)(k_{31}^z + s)}{f(s)} , \tag{A4}$$

where

$$\begin{aligned} f(s) = {} & (K_2 + 2w + s)(k_{31}^x + s)(k_{31}^y + s)(k_{31}^z + s) \\ & + wk_{23}^x(k_{31}^y + s)(k_{31}^z + s) + wk_{23}^y(k_{31}^x + s)(k_{31}^z + s) \\ & + wk_{23}^z(k_{31}^x + s)(k_{31}^y + s) . \end{aligned} \tag{A5}$$

To make the inverse Laplace transformation feasible, $n_2(s)$ has to be written in the following form:

$$\begin{aligned} n_2(s) &= wN_0\left(\frac{(k_{31}^x + s)(k_{31}^y + s)(k_{31}^z + s)}{s(s - s_1)(s - s_2)(s - s_3)(s - s_4)}\right) \\ &= wN_0\left(\frac{c_0}{s} + \frac{c_1}{s - s_1} + \frac{c_2}{s - s_2} + \frac{c_3}{s - s_3} + \frac{c_4}{s - s_4}\right) . \end{aligned} \tag{A6}$$

Here s_1 through s_4 are the roots of the equation

$$f(s) = 0 \tag{A7}$$

The coefficients c_0 through c_4 are obtained using the theory of partial fractions.[29] For example,

$$c_1 = \left(\frac{(k_{31}^x + s)(k_{31}^y + s)(k_{31}^z + s)}{s(s - s_2)(s - s_3)(s - s_4)}\right)_{s=s_1} . \tag{A8}$$

Thus we have to solve Eq. (A7). This is a quartic (or biquadratic) equation. Such an equation is just still solvable analytically,[75] in principle. However, in our case this yields very lengthy expressions. The calculations to obtain theoretical results that can be compared with the experimental fluorescence transients, would be performed numerically (Secs. III B and III G). The procedure given in Ref. 75 for solving the quartic equation, was included by us in a computer program to simulate the fluorescence transients.

The final result for $N_2(t)$ has the form

$$N_2(t) = wN_0(c_0 + c_1 e^{s_1 t} + c_2 e^{s_2 t} + c_3 e^{s_3 t} + c_4 e^{s_4 t}) . \tag{A9}$$

APPENDIX B. CALCULATION OF THE PENTACENE CONCENTRATION IN THE CRYSTALS USED

In this calculation we use the formalism, treated by Loudon[76] (m.k.s. units). For the light attenuation across the sample we have

$$I(z) = I_0 \exp(-Kz) , \tag{B1}$$

where $I(z)$ and I_0 are the intensities of the light leaving the crystal (thickness z) and incident upon it, respectively. K is the absorption coefficient in m^{-1}. For K the following formula can be derived[76]:

$$K = \frac{NB\hbar\omega F(\omega)}{Vcn} . \tag{B2}$$

Here N is the total number of absorbing molecules in the inhomogeneous absorption line considered, B is the Einstein B coefficient, $F(\omega)$ is the inhomogeneous line shape normalized to unit area, V is the volume of the

part of the crystal that was used, c the velocity of light in vacuum, and n the refractive index of the crystal.

It is important to note here that Eq. (B2) was derived in Ref. 76 for a two-level system. However, as in molecular OFID[24] and for the fluorescence transients treated in the present paper, also in the derivation of the absorption coefficient formula (B2) the lowest triplet state T_1 has to be considered. We will only take into account here one spin-sublevel. In Ref. 76 the approximation $2B\overline{W}/A \ll 1$ is made, which is assumed to hold for ordinary (chaotic) light beams. Here $\overline{W}$ is the radiation field mean energy density and A the Einstein coefficient for the spontaneous emission $|1\rangle \leftarrow |2\rangle$ ($S_0 \leftarrow S_1$). Taking into account the intermediate triplet level ($|3\rangle$) and the radiationless process $S_0 \leftarrow S_1$ the approximation needed to derive Eq. (B2) becomes

$$\frac{\left(2+\frac{k_{23}}{k_{31}}\right)B\overline{W}}{A+k_{21}+k_{23}} \ll 1 ,$$

where A is still the Einstein coefficient, k_{23} is the $T_1 \leftarrow S_1$ ISC rate, k_{31} the $S_0 \leftarrow T_1$ ISC rate and k_{21} the $S_0 \leftarrow S_1$ internal conversion rate. For the lower pentacene sites in p-terphenyl $k_{23}/k_{31} \cong 8$, and the approximation will still hold for ordinary light beams. For other molecules k_{23}/k_{31} may be as high as 10^6. In such a case the approximation will in general not be valid and the formalism describing the absorption becomes different.

We proceed with the consideration of the lower pentacene sites. As in our absorption experiments unpolarized light was incident on the p-terphenyl crystal ab plane, K can be considered to consist of two contributions:

$$K=\frac{N\hbar\omega F(\omega)}{Vc}\left(\frac{B_b}{n_b}+\frac{B_a}{n_a}\right) , \tag{B3}$$

where the a, b subscripts refer to the respective crystal axes. For the isotropic case one can derive[76]:

$$B=\frac{\pi|\mu|^2}{3\epsilon_0\hbar^2} . \tag{B4}$$

For our case the appropriate formula is

$$B_b=\frac{\pi\mu^2\cos^2\theta}{\epsilon_b\hbar^2} , \tag{B5}$$

where θ is the angle between the pentacene short molecular axis and the crystal b axis. ϵ_b is the crystal permittivity along the b axis. A similar formula holds for B_a. By a rearrangement of terms in Eq. (B3), and integration over ω, one gets[76]:

$$\int\frac{Kc}{\hbar\omega}\,d\omega=\frac{N}{V}\left(\frac{B_b}{n_b}+\frac{B_a}{n_a}\right) , \tag{B6}$$

where n_a and n_b are taken to be constant across the inhomogeneous line. As B_b and B_a are known from the obtained μ value, and $K(\omega)$ can be deduced from the measured absorption spectrum, we are able to calculate the real concentration (N/V in number per m^3) of pentacene molecules. From (B1) we have:

$$K=\frac{1}{z}\ln\frac{I_0}{I(z)}\simeq\frac{1}{z}\frac{I_0-I(z)}{I_0} . \tag{B7}$$

$I_0-I(z)/I_0$ is just the amount of absorption, measured as a function of frequency. Expression (B7) holds for small absorption values. We will calculate N/V for the O_1 site (proto). The amount of absorption at the top of the line was 0.17 (Table III), while the line shape was Gaussian to a good approximation. Therefore K has a Gaussian shape with a maximum of $K_{max}=(1/z)\times 0.17 = 2.88\times10^2\ m^{-1}$. The left-hand side of (B6) now becomes

$$\int_0^\infty\frac{Kc}{\hbar\omega}\,d\omega=\frac{cK_{max}}{\hbar}\int_0^\infty\frac{1}{\omega}\exp\left[-\left(\frac{2\sqrt{\ln 2}(\omega-\omega_c)}{\Delta\omega_G}\right)^2\right]d\omega . \tag{B8}$$

Here $\Delta\omega_G$ can be obtained from Table III. Now, as ω varies little across the region, where K has an appreciable value, we may take the factor $1/\omega$ outside the integral. The result becomes

$$\int_0^\infty\frac{Kc}{\hbar\omega}\,d\omega=3.62\times10^{40}\ J^{-1}\,s^{-2} . \tag{B9}$$

As $\epsilon_b/\epsilon_0=2.85$, $\epsilon_a/\epsilon_0=2.58$, $n_b=1.69$, and $n_a=1.61$,[77] we calculate

$$\frac{B_b}{n_b}+\frac{B_a}{n_a}=3.90\times10^{19}\ J^{-1}\,s^{-2}\,m^3 . \tag{B10}$$

Thus, finally, from (B6)

$$N/V=9.3\times10^{20}\ \text{molecule}/m^3 ,$$

where it should be recalled that N is the total number of molecules giving the inhomogeneous absorption line. This means a pentacene concentration relative to that of p-terphenyl (taking for this host a density of 1) of $(3.6\ ^{+5.5}_{-1.6})\times10^{-7}$ mol/mol.

Note added While this manuscript was being completed, we received a copy of a manuscript by Orlowski and Zewail[78] in which they also analyze the fluorescent transient of pentacene in p-terphenyl. We note that their interpretation of the transient is now in agreement with ours. They obtained for the lower (O_1, O_2) sites (proto) an ISC yield from S_1 of 0.12% to 0.20%, which is somewhat lower than the values obtained in our work. From the transient nutation they obtained for the $S_1 \leftarrow S_0$ transition a dipole moment $\mu=0.7\pm0.1$ D, which agrees within experimental error with our earlier result (0.9 ± 0.3 D).[24]

Note added in proof: Recently we noticed that, at the laser power level used in our fluorescence-transient experiments, the power broadening term in the expression for the induced transition rate w should have been included. Inclusion of this term changes Eq. (11) into

$$w=\left(\frac{T_2}{2}\chi^2\right)\Big/\left(T_2^2\Delta^2+1+\tfrac{1}{2}T_2^2\chi^2\right) ,$$

where $\chi=\mu_{12}E_0/\hbar$ and $\Delta=\omega-\bar{\omega}_0$. All the numbers appearing in this article have been calculated using the correct expression for w, with one exception: all the values of the quantity w_{max} in this paper were calculated according to the definition in Eq. (13).

ACKNOWLEDGMENTS

We are indebted to Spectra-Physics Benelux b. v. for lending us a 165 Ar-ion laser. We are also grateful to Drs. J. B. W. Morsink for his assistance in the fluorescence lifetime measurements. The investigations

were supported by the Netherlands Foundation for Chemical Research (SON).

[1]H. de Vries, P. de Bree, and D. A. Wiersma, Chem. Phys. Lett. **52**, 399 (1977); Erratum **53**, 418 (1978).
[2]H. de Vries and D. A. Wiersma, Proceedings of the Conference on Dynamical Processes in the Excited States of Ions and Molecules in Solids (Athens, Georgia, USA, June 2–3, 1978), communication C 2.
[3]A. H. Zewail, T. E. Orlowski, and K. E. Jones, Proc. Natl. Acad. Sci. USA **74**, 1310 (1977).
[4]A. H. Zewail, K. E. Jones, and T. E. Orlowski, Spectrosc. Lett. **10**, 115 (1977).
[5]R. G. Brewer and A. Z. Genack, Phys. Rev. Lett. **36**, 959 (1976).
[6]T. J. Aartsma and D. A. Wiersma, Chem. Phys. Lett. **42**, 520 (1976).
[7]J. B. W. Morsink, T. J. Aartsma, and D. A. Wiersma, Chem. Phys. Lett. **49**, 34 (1977).
[8]T. E. Orlowski, K. E. Jones, and A. H. Zewail, Chem. Phys. Lett. **54**, 197 (1978).
[9]K. F. Freed and J. Jortner, J. Chem. Phys. **52**, 6272 (1970).
[10]B. R. Henry and W. Siebrand, in *Organic Molecular Photophysics*, edited by J. B. Birks (John Wiley & Sons, New York, 1973), Vol. 1, p. 153.
[11]J. Jortner and S. Mukamel, in *The World of Quantum Chemistry*, edited by R. Daudel and B. Pullman (D. Reidel, Dordrecht, 1974), p. 145.
[12]K. F. Freed, Top. Appl. Phys. **15**, 23 (1976).
[13]J. Jortner, S. A. Rice, and R. M. Hochstrasser, Adv. Photochem. **7**, 149 (1969).
[14]K. F. Freed and J. Jortner, J. Chem. Phys. **50**, 2916 (1969).
[15]K. F. Freed, J. Chem. Phys. **52**, 1345 (1970).
[16]A. Nitzan and J. Jortner, Theor. Chim. Acta **29**, 97 (1973).
[17]A. Nitzan and J. Jortner, Theor. Chim. Acta **30**, 217 (1973).
[18]F. Lahmani, A. Tramer, and C. Tric, J. Chem. Phys. **60**, 4431 (1974).
[19]H. de Vries and D. A. Wiersma, Phys. Rev. Lett. **36**, 91 (1976).
[20]H. de Vries and D. A. Wiersma, Chem. Phys. Lett. **51**, 565 (1977).
[21]Note that for a general molecular singlet, triplet level system the relation between T_2 (decay time of the off-diagonal elements of the density matrix) and the population decay rates cannot simply be derived using the treatment of M. Sargent III, M. O. Scully, and W. E. Lamb, Jr. in *Laser Physics* (Addison-Wesley, Reading, Mass., 1974), Ch. 7. We want to stress here the usefulness, for the description of *intra*-molecular closed pumping cycles, of the density matrix equation of motion given by W. G. Breiland, M. D. Fayer, and C. B. Harris, Phys. Rev. A **13**, 383 (1976):

$$\dot{\rho} = \frac{1}{i\hbar}[H,\rho] - \{K,\rho\} + F,$$

where $\{\ldots\}$ denotes anticommutation. When the decay matrix K and the feeding matrix F are chosen phenomenologically in such a way that the diagonal element equations obtain their proper decay and feeding terms, the result is that $T_2 = 2\tau_{f1}$ (when the molecule–bath interaction can be ignored).
[22]B. de Bartolo, *Optical Interactions in Solids* (Wiley, New York, 1968), pp. 431–442.
[23]J. H. Meyling and D. A. Wiersma, Chem. Phys. Lett. **20**, 383 (1973).
[24]H. de Vries and D. A. Wiersma, J. Chem. Phys. **69**, 897 (1978).
[25]P. de Bree and D. A. Wiersma, Opt. Commun. **26**, 248 (1978).
[26]W. Hartig and H. Walther, Appl. Phys. **1**, 171 (1973).
[27]J. B. Birks, *Photophysics of Aromatic Molecules* (Wiley-Interscience, London, 1970), Chaps. 5 and 6.
[28]S. I. Weissman and S. S. Kim (to be published).
[29]*Handbook of Chemistry and Physics*, 47th ed. (Chemical Rubber, Cleveland, Ohio, 1966), p. A236.
[30]W. H. Louisell, *Quantum Statistical Properties of Radiation* (Wiley, New York, 1973), Chap. 5.
[31]L. Allen and J. H. Eberly, *Optical Resonance and Two-Level Atoms* (Wiley, New York, 1975).
[32]W. G. van Dorp, W. H. Schoemaker, M. Soma, and J. H. van der Waals, Mol. Phys. **30**, 1701 (1975).
[33]P. A. Chiha and R. H. Clarke, J. Magn. Reson. **29**, 535 (1978).
[34]W. R. Leenstra, M. Gouterman, and A. L. Kwiram, J. Chem. Phys. **68**, 327 (1978).
[35]M. A. El-Sayed, Ann. Rev. Phys. Chem. **26**, 235 (1975).
[36]M. A. El-Sayed and R. Leyerle, J. Chem. Phys. **62**, 1579 (1975).
[37]R. L. Barger, M. S. Sorem, and J. L. Hall, Appl. Phys. Lett. **22**, 573 (1973).
[38]R. L. Barger, J. B. West, and T. C. English, Appl. Phys. Lett. **27**, 31 (1975).
[39]J. H. Meyling, W. H. Hesselink, and D. A. Wiersma, Chem. Phys. **17**, 353 (1976).
[40]L. W. Pickett, Proc. R. Soc. Sect. A **142**, 333 (1933).
[41]J. L. Baudour, Y. Delugeard, and H. Cailleau, Acta Crystallogr. Teil B **32**, 150 (1976).
[42]J. H. Meyling, P. J. Bounds, and R. W. Munn, Chem. Phys. Lett. **51**, 234 (1977).
[43]J. H. Meyling (unpublished results).
[44]B. Soep, Chem. Phys. Lett. **33**, 108 (1975).
[45]C. Hellner, L. Lindqvist, and P. C. Roberge, Faraday Trans. II **68**, 1928 (1972).
[46]R. E. Merrifield, J. Chem. Phys. **23**, 402 (1955).
[47]R. G. DeVoe and R. G. Brewer, Phys. Rev. Lett. **40**, 862 (1978).
[48]A. Brillante and D. P. Craig, Faraday Trans. II **71**, 1457 (1975).
[49]J. B. W. Morsink (unpublished results).
[50]A. Z. Genack and R. G. Brewer, Phys. Rev. A **17**, 1463 (1978).
[51]H. de Vries (unpublished results).
[52]Landolt-Börnstein, *Zahlenwerte und Funktionen*, 6th ed., (Springer, Berlin, 1962), Vol. II, Part 8, p. 2–287.
[53]R. Pariser, J. Chem. Phys. **24**, 250 (1956).
[54]T. E. Peacock and P. T. Wilkinson, Proc. Phys. Soc. **83**, 525 (1964).
[55]G. G. Hall, Proc. R. Soc. Sect. A **213**, 113 (1952).
[56]D. R. Kearns, J. Chem. Phys. **36**, 1608 (1962).
[57]N. E. Geacintov, J. Burgos, M. Pope, and C. Strom, Chem. Phys. Lett. **11**, 504 (1971).
[58]R. E. Kellogg, J. Chem. Phys. **44**, 411 (1966).
[59]P. F. Jones and S. Siegel, Chem. Phys. Lett. **2**, 486 (1968).
[60]E. J. Bowen and J. Sahu, J. Phys. Chem. **63**, 4 (1959).
[61]R. G. Bennett and P. J. McCartin, J. Chem. Phys. **44**, 1969 (1966).
[62]B. Soep, A. Kellmann, M. Martin, and L. Lindqvist, Chem. Phys. Lett. **13**, 241 (1972).
[63]W. Siebrand and D. F. Williams, J. Chem. Phys. **49**, 1860 (1968).
[64]B. Sharf and R. Silbey, J. Chem. Phys. **53**, 2626 (1970).
[65]F. Tanaka and J. Osugi, Chem. Phys. Lett. **27**, 133 (1974).
[66]J. Ferguson and A. W.-H. Mau, Mol. Phys. **28**, 469 (1974).
[67]P. F. Jones and A. R. Calloway, *Transitions Nonradiatives dans les Molécules*, J. Chim. Phys. (Paris, 1969), p. 110.
[68]A. Kearvell and F. Wilkinson, *Transitions Nonradiatives dans les Molécules*, J. Chim. Phys. (Paris, 1969), p. 125.
[69]W. R. Ware and B. A. Baldwin, J. Chem. Phys. **43**, 1194 (1965).
[70]E. C. Lim, J. D. Laposa, and J. M. W. Yu, J. Molec. Spectrosc. **19**, 412 (1966).

[71]E. R. Pantke and H. Labhart, Chem. Phys. Lett. **16**, 255 (1972).
[72]Y. H. Meyer, R. Astier and J. M. Leclercq, J. Chem. Phys. **56**, 801 (1972).
[73]W. H. Hesselink and D. A. Wiersma, *Picosecond Phenomena*, edited by C. V. Shank, E. P. Ippen and S. L. Shapiro, Springer Series in Chemical Physics, Vol. 4 (Springer, Berlin, 1978), p. 192.
[74]S. Völker and R. M. Macfarlane, Abstracts of the International Conference on Luminescence, Paris, 1978; and Chem. Phys. Lett. 61, 421 (1979).
[75]H. W. Turnbull, *Theory of Equations* (Oliver & Boyd, Edinburgh/London, 1957), Chap. X.
[76]R. Loudon, *The Quantum Theory of Light* (Clarendon, Oxford, 1973), Chaps. 2 and 3.
[77]J. H. Meyling, thesis, Groningen, 1977.
[78]T. E. Orlowski and A. H. Zewail, J. Chem. Phys. 70, 1390 (1979).